

The Development of a Laser-Illuminated Infrared Imager for Natural Gas Leak Detection

Thomas J. Kulp (tjkulp@sandia.gov; (510) 294-3676)
Peter E. Powers (pepower@sandia.gov; (510) 294-2696)
Randall Kennedy ((510) 294-1343)
Sandia National Laboratories
P.O. Box 969 MS 9057
Livermore, CA 94551-0969

INTRODUCTION

In this co-funded DOE/GRI project a new technology is being developed to detect and locate natural gas leaks. The method, called backscatter absorption gas imaging (BAGI), uses laser active imaging to generate video imagery of gas plumes that are not visible to the eye. The basic concept is quite simple— an area is illuminated with infrared laser radiation as it is imaged by an infrared camera. The laser is tuned to a wavelength that is absorbed by the gas to be detected. Thus, if a gas plume is present in the imaged zone, it attenuates some of the backscattered laser light and causes a dark cloud to appear in the video picture. A differential mode of detection is being developed as well, in which frames taken at two different laser wavelengths (one absorbed and one not absorbed by the gas) are processed to generate a transmittance image of the scene. This removes all scene information except that of the gas plume, thereby making it more visually apparent. The primary benefit of imaging for leak detection is its ability to instantaneously sense gas leaks at any point within a large area. It offers a significant increase in speed and effectiveness over that attainable with state-of-the-art leak survey detectors. This has particular relevance to the gas industry, where complex or extensive gas piping networks are mandated to be routinely surveyed for leaks. Potential benefits include: (1) significant reduction in survey costs; (2) minimization of gas lost to leaks; and (3) further enhancement of the achievable level of safety within the gas industry. Industry-wide reductions in methane emissions would accelerate the attainment of several national goals such as energy conservation and the mitigation of global warming. Development of this technology for natural gas detection will lead to its further extension to the detection of other harmful or toxic gases and vapors in the environment.

It is anticipated that BAGI instrumentation could operate from a stationary and/or a moving platform. The latter might include van-mounted systems for application in local utilities, or aerial-mounted systems for surveys of transmission pipelines. The remote sensing capability of BAGI would also facilitate the inspection (from a stationary platform) of gas processing equipment and above-ground piping at locations such as metering stations, regulator stations, compressor stations, and LNG and storage facilities. Ultimately, it may also be possible to build a man-portable version of the imager that could be used in a similar manner to a video camcorder.

OBJECTIVES

The general objective of this project is the development of a BAGI imager that has sufficient standoff range and natural gas detection sensitivity to be useful to the natural gas industry. The application of highest interest is the detection of leaks during routine surveys of natural gas distribution

systems in residential or industrial areas. This constitutes the most costly leak-sensing operation and, thus, the area of greatest potential cost savings. In order for a van-mounted BAGI imager to be useful for distribution surveys it must have a standoff range sufficient to allow it to image at the maximum expected distance from the road to the residential or industrial service. This is assumed to be ~40 m. The minimum required gas sensitivity is more difficult to specify. Flame-ionization detectors (FIDs) now widely used in the industry exhibit threshold sensitivities to natural gas of approximately 1-4 ppm. The surface concentration of natural gas resulting from a below-ground leak varies widely as a function of position on the surface. Discussions with Pacific Gas and Electric (PG&E) survey teams indicate that the *peak* surface concentration exhibited by the smallest categorized leak is typically ~100 - 700 ppm. Although this is many times the sensitivity threshold of an FID, the excess sensitivity of the sniffer is necessary because it allows a leak to be detected at some distance from its point of maximum intensity. Leak survey teams exploit this sensitivity to allow them to scan an area with only a finite number of "sniffs". Nonetheless, it is possible that these measurements may still miss a leak. The imager, in contrast, samples all points in its field-of-view. The sensitivity to natural gas (methane) of the BAGI imager under development is approximately 7-10 ppm-m (the units arise because BAGI measures a path-integrated absorption; i.e., a 7 ppm-m sensitivity indicates 7 ppm can be detected for a 1-m plume, 14 ppm is the threshold for a 0.5-m plume, etc). Thus, its point sensitivity is less than that of the sniffer—however, its large area of influence makes it more likely to sample the region of highest concentration. Its threshold sensitivity is expected to be high enough to allow it to detect all required leaks at the maximum concentration point. A second objective of this project is to field-test the sensitivity of BAGI in detecting gas percolating to the surface from realistic buried leak sources and to compare the performance of BAGI to that of an FID. This will be done in both controlled tests and in tests at leaks in distribution systems that have been identified by gas utility companies.

APPROACH

Two approaches have been taken to develop a BAGI imager that meets the needs of the gas industry. One focuses on the development of a new implementation of BAGI that uses fundamentally different instrumentation than earlier BAGI systems. The second path involves the development of a new laser that will allow the original BAGI instrumentation to operate at the required range and sensitivity. Both build upon earlier work performed for GRI by Laser Imaging Systems (LIS - Punta Gorda, FL) in which the original BAGI system was applied to natural gas detection. That system was demonstrated to successfully image methane in controlled tests and in field trials at natural gas compressor stations and distribution systems. It was, however, found to be limited to short (6 m) range operation and could not image at the maximum absorbing wavelength. That system will be referred to as the "scanned" imager because it operates by scanning a continuous-wave (cw) laser across the scene in a raster-pattern as the scene is imaged by a scanning infrared video camera. In its implementation by LIS, the range and sensitivity limitations stem from its of the infrared helium-neon (HeNe) laser source. The HeNe provides relatively low (30 mW) power of light at a single wavelength that is coincident with an absorption that is about one-third as strong as that of the maximum methane absorption. The infrared HeNe is, however, the highest-power fieldable source suitable for natural gas detection that is commercially available in the cw format required by the scanned imager.

Limitations in the performance of the HeNe-based scanner motivated the development of the new implementation of BAGI which employs a pulsed laser source to illuminate the scene and a focal-plane array (FPA) camera to image the laser-illuminated scene. Operation in the pulsed mode has several

advantages. Mid-infrared lasers are more readily available in the pulsed mode because nonlinear frequency conversion can be used to shift the wavelength of high power, near-infrared light sources into the mid-infrared. Nonlinear conversion relies on high peak power and is not typically as efficient in the cw mode. Several options exist for high (0.2-1 W) average power pulsed laser sources that operate in the region of the infrared (near 3.3 μm) in which methane absorbs. The high power, combined with the increased light-collection efficiency and lower noise afforded by infrared FPA cameras, makes it possible for the pulsed imager to exceed the standoff range goals required in distribution surveys. Moreover, pulsed lasers generate wavelength-tunable emissions which allow their output wavelength to be adjusted to the peak of the methane absorption spectrum. The fixed-frequency output of the infrared HeNe limited sensitivity of the original scanned system to ~ 20 ppm-m, while that of an optimized pulsed imager can be as low as 7 ppm-m. As will be discussed later in this document, the tunability of the pulsed mode also allows differential imaging, in which image processing is employed to enhance the visibility of small gas leaks.

A two-step plan was formulated to develop the pulsed imager. In the first step, a breadboard imager would be assembled to demonstrate feasibility of the pulsed concept. Given success of the first step, the second phase would involve the development of a compact, fieldable prototype pulsed imager. The first step was initiated at the start of FY95 and reached successful completion during August of FY96. The pulsed imager was found to image at ranges up to ~ 90 m at wavelengths that are coincident with the peak absorption of methane. At that point, the second phase began. A design was formulated for a compact pulsed optical parametric oscillator (OPO) that would be suitable for a prototype pulsed imager. Upon completion of this design, however, a new capability in high-power, mid-IR cw laser sources became available. This was enabled by the development of the nonlinear material periodically-poled lithium niobate (PPLN). The attributes of PPLN make it possible, for the first time, to assemble a cw OPO having sufficient power (up to 1 W) to allow long-range imaging of natural gas with the first generation scanned imager. The PPLN OPO also offers broad tunability to allow optimization to the methane absorption peak. A trade comparison of the scanned and pulsed approaches was then made, in light of the new development. It was determined that the cw approach would now allow a more rugged, low-cost, and compact format than the pulsed design, although at some expense in image resolution. At that point, Sandia began work on the development of PPLN laser source for a prototype scanned BAGI imager. This is the second approach mentioned above.

The FY97-8 work involves several activities—(1) development of a fieldable PPLN laser source for use in a scanned imager (to be supplied by LIS), (2) support of field-testing of that laser source, (3) field-testing of the breadboard pulsed imager, and (4) further refinement of the differential imaging technique. Field testing involves imaging controlled buried leak sources and imaging "real-world" leaks identified by local utility companies. Although the pulsed imager is not being taken to the prototype stage, it will be used in field tests because it provides higher image quality and resolution than the scanner. Its performance will indicate the level of image quality that could be obtained with a future improved scanner.

TECHNOLOGY

Description of the scanned BAGI imager

Figure 1 contains a diagram that illustrates the operation of the first-generation scanned BAGI imager. It consists of a flying-spot infrared imaging radiometer that was modified to scan the beam of a

cw laser in synchrony with the scan of the instantaneous field-of-view (IFOV) of its single-element infrared detector. As indicated in the figure, the scan occurs in a raster pattern that is carried out at video rates, thus providing a real-time laser-illuminated image of the scene. The device that produces the raster scan consists of a pair of galvanometrically-swept scan mirrors. The horizontal mirror operates at a scan rate of 3933 Hz, providing the horizontal dimension of the video image while the vertical mirror sweeps at a frequency of 60 Hz, to produce the vertical dimension of the picture. The combined motion of the two mirrors produces the raster scan. The dimensions of the system field-of-view can be varied up to a full scan angle of 18° in the horizontal dimension. More specific details regarding the imager hardware are provided in Refs. 1-4.

The scanned BAGI imager was converted by LIS to allow it to operate with a 3.39 μm wavelength HeNe laser source. That imager was demonstrated to image methane at concentrations as low as 20 ppm-m and was successfully tested at a number of above- and below-ground leak locations. These included (1) a test at a sensor intercomparison trial coordinated by Pacific Gas and Electric (PG&E) involving the detection of leaks in below-ground pipes pressurized to 50 psi with natural gas, (2) a demonstration of the ability to image below-ground Class 3 or 4 leaks located in residential natural gas distribution systems at Charleston, SC and Sarasota, FL, and (3) a demonstration of the ability to image above-ground leaks at compressor stations in Orlando, FL.

While extremely successful at short-range leak detection, the imager was found to be limited in certain aspects of its performance:

- (1) The range was limited to 6-m because of the low power (30 mW) of the IR helium neon laser. This is the highest power cw laser that is currently available that operates at a methane absorption line. The scanned imager must operate with a cw laser.
- (2) Range is also limited because the optical collection aperture of the scanner is constrained to a diameter of 1.2 cm, which is the size of the horizontal scan mirror. The aperture diameter determines the amount of light that is collected.
- (3) The field-of-view of the imager cannot exceed 18 degrees, which is the maximum amplitude of the horizontal scan mirror.
- (4) The spatial resolution of the imager is limited because the imager cannot achieve a true optical zoom. An effective zoom is accomplished by reducing the amplitude of the scan mirror motion. However, although this reduces the field-of-view, the size of the laser spot and IFOV remain the same. Thus, the spatial resolution is not increased when zooming the image field-of-view.

Limitations in range, resolution, and field-of-view directly influence the ability of the imager to rapidly search for gas leaks. Recognition of these limitations motivated the development of the pulsed laser imager.

Description of the pulsed BAGI imager

Figure 2 contains a diagram of the breadboard pulsed imager developed in this project. The apparatus consists of three components: a pulsed tunable infrared laser source, a beam

formatter/projector, and a synchronously-gated focal plane array camera. The laser is a bench-scale device that was used because of its availability. In the fieldable prototype, it was intended to be replaced by a compact optical parametric oscillator (OPO). The laser consists of a lithium niobate difference frequency generation (DFG) stage followed by a lithium niobate optical parametric amplification (OPA) stage. A Nd:YAG laser is used to pump a dye laser. The output of the dye laser and the Nd:YAG are mixed in the lithium niobate DFG crystal to generate 7 nsec IR pulses having a wavelength that is tunable between 3.2 and 3.7 μm . The rate of pulse generation is 30 Hz. These pulses are amplified in the lithium niobate OPA crystal by mixing with additional Nd:YAG radiation to generate the final pulse energy of approximately 5 mJ per pulse at an approximate linewidth of $\sim 1 \text{ cm}^{-1}$. The pump source for both the DFG and the OPA is an injection-seeded Nd:YAG laser emitting 600 mJ pulses at a 30 Hz repetition rate.

Tuning of the infrared light is accomplished by changing the dye laser grating and by adjusting the crystal angles. In addition to gross tuning, the laser is also capable of operating in a "dither mode" in which the infrared output wavelength rapidly (33 msec switching time) jumps back and forth between two preset values. The spacing of these wavelengths can vary between ~ 1 and 25 cm^{-1} . The system was adapted to allow dither mode by installing a piezoelectric translator on the dye laser grating and by mounting the DFG and OPA crystals on galvanometers.

Uniform spatial formatting of the laser radiation onto the target is critical in a full-field illuminated imager. This was accomplished using a beam-homogenizer/projector assembly, illustrated in Figure 3. A ZnSe beam expander directs a collimated beam onto a ZnSe faceted lens. The faceted lens is equivalent to a prism array and consists of 16 $1/4$ " facets and 16 partial facets around the edge of the lens on a 1.5" diameter with an effective f-number of 1.7. The faceted lens segments the expanded beam and then overlaps these segments at a distance of 2.5" from the surface of the lens. A ZnSe f/1.7, 3.3" focal-length lens images the overlap region onto the target. This projection lens was designed to fill a 5° field-of-view and minimize edge blurring.

The camera (Amber Model AE-173) is based on a modified cooled InSb 256x256 array having a snapshot-mode, direct-injection (DI) readout. The array is housed in a pour-cooled liquid nitrogen dewar that is typically operated at 77K, but can be evacuated to reach temperatures near 65K. In a prototype, this could be replaced by a compact mechanical chiller. The camera was fitted with an f/1, 88-m e.f.l. lens, giving it a field-of-view (5°) matched to that of the laser projection optics. A cold filter installed in the camera limited collected radiation to a bandpass of 0.5 μm centered at $\sim 3.31 \mu\text{m}$. This is positioned at the peak of the methane Q-branch absorption, the frequency to which the laser was tuned.

The camera was controlled by the Amber ProView system, a universal FPA driver that allows user-programmable FPA exposure and readout. The laser was triggered by a ProView clock output at a rate of 30Hz. The camera was clocked at a frame rate of 90 Hz in a repetitive three frame operation referred to as the "bias-sum-subtract" mode. During the first frame of the operation, a digital frame buffer is filled with an array of identical positive numerical values (thereby "biasing" the buffer with non-zero values). During the second frame a passive scene image is recorded by the FPA and summed to the buffer. The final frame is synchronized with the firing of the laser. In that frame an active-plus-passive image is recorded by the FPA and subtracted from the buffer. At the end of the three-frame cycle, the numerical remainder in the buffer represents a biased active-only image. Only this image is displayed on the screen, at a refresh rate of 30 Hz. The FPA is snapshot-gated on during both the second

and third frames of the sequence (with a width adjustable between 1 and 1100 μs). The collected imagery can be displayed in real-time and recorded directly to digital memory or onto analog (S-VHS) videotape.

As indicated above, some modifications were made to the standard AE-173 FPA and camera. These were: (1) reduction of the unit cell integration capacitor from $\sim.4$ to $.1$ pF; (2) hand-selection of the InSb diode array to allow operation at a reverse-bias of 1V with a mean dark current of 81 pA at 65 and a mean dark current of 260 pA at 77K; and (3) use of a dewar compatible with f/1 rather than f/2 optics. It was necessary to make these changes because standard FPA cameras are optimized for the detection of high levels of continuous thermal radiation, and not short pulse laser radiation. High array bias is necessary to prevent saturation of the array at short ranges. Reduction in capacitor size and in the f-number is necessary to more efficiently sense the low light levels that are detected in the laser imaging application.

Description of the PPLN OPO

As indicated above, PPLN is a novel nonlinear optical material that has recently become available and which allows infrared laser sources to be made that were not possible in the past. The unique feature of PPLN is that its nonlinear properties can be engineered (via an electric-field poling process) to allow nonlinear conversion over a much broader wavelength range and at much higher efficiencies than is possible in ordinary lithium niobate. This is important to gas imaging because it allows narrowband (0.1 cm^{-1}) cw infrared radiation to be generated in a high power ($\sim 0.5\text{-}1\text{ W}$) continuously-tunable format in the $1.3\text{-}4.5\text{ }\mu\text{m}$ wavelength range. This is an extremely useful laser for scanned BAGI imaging of natural gas and many other organic species.

Figure 4 contains a diagram of the PPLN OPO that has been assembled in a breadboard format. This laser will be used in field tests in collaboration with LIS during the summer of FY97. The OPO is pumped by a nominal 9.5W cw Nd:YAG laser beam that is focused into the PPLN crystal. The crystal is contained in the bowtie ring OPO cavity, defined by the two flat (M1, M2) and two spherical (M3, M4) mirrors. The OPO generates two laser beams, called the signal and the idler, whose frequencies add up to the frequency of the Nd:YAG laser. The signal beam is resonated within the OPO cavity, while the Nd:YAG pump and the idler are allowed to pass out of the cavity at M4. The idler beam is used as the gas imaging illumination source. Gross frequency control of the OPO is accomplished by translating various regions of the PPLN crystal into the cavity. Fine control is achieved by rotating two intracavity etalons (E1 and E2). These control mechanisms determine the wavelength of the resonated signal and, thus, the idler as well. The output linewidth of the signal is less than 1 MHz, while the idler linewidth is approximately 5 GHz (equal to that of the pump laser). The idler output power is $\sim 0.5\text{ W}$ and that of the signal is $\sim 1.5\text{ W}$.

During initial field testing, the idler wavelength will be set to the Q-branch absorption of methane ($3.31\text{ }\mu\text{m}$). The Q-branch feature was chosen because it is broad, thereby reducing the precision of laser frequency control required. The OPO will be maintained at the correct wavelength via manual frequency control. A portion of the idler beam will be split off and sent into a cell containing methane. The ratio of the power leaving the cell to that entering is displayed on a digital readout. The etalons will be periodically adjusted to minimize this ratio, thus keeping the laser at the peak of the absorption. In the future, the frequency control may be automated using an electronic locking mechanism.

RESULTS

Following its assembly, the ability of the pulsed imager to visualize controlled-flowrate, point-source methane leaks was evaluated. Three parameters were explored — the imaging range, the minimum detectable natural gas flowrate, and the performance of the imager in the differential imaging mode. Imaging range was determined by viewing a surface of known infrared reflectivity at several ranges. The imager was mounted to view horizontally out of the rear of a vehicle; the target surface was mounted vertically on a platform that could be moved with respect to the vehicle. The target surface was composed of a diffusely-reflecting silicon carbide abrasive paper having a comparable reflectivity to that of many terrestrial surfaces. Methane leaks of known flowrate were created in front of the target panel using a rotometer.

During the tests, the imager-to-target range was varied between 30 and 100 m. Figure 5 contains an image created at a range of 20 m and a flowrate of 0.2 standard cubic feet per hour (scfh). Methane leaks having a flowrate of 0.2 scfh were visually detectable at ranges up to 80 m. In separate tests conducted indoors at ranges of a few meters, leaks as low as 0.02 scfh were visible.

The signal and noise properties of the collected images were compared to those predicted by an electro-optical model that was formulated during the imager development. The model calculates the expected return laser return signal (in electrons per pixel per frame) and the expected noise level (in the same units) as a function of imaging range. Noise sources incorporated into the model include laser and thermal photon shot noise, array read noise, array dark current noise, analog-to-digital conversion noise, and noise due to laser speckle. Laser speckle is an interference effect that gives laser light its "grainy" appearance. It is assumed that the range limit occurs at the point where the laser backscatter signal-to-noise ratio is reduced to a level of 12, as this is the point where an 8% attenuation of the laser radiation would be equal to the noise level. An attenuation of this magnitude is caused by a methane density of ~12 ppm-m when operating at the laser wavelength and bandwidth used in the tests. The use of a narrower bandwidth laser would reduce the minimum detectable density to about 7 ppm-m.

Figure 6 contains plots of the calculated and measured laser return signal and signal-to-noise ratio as a function of range. Measured levels were extracted from the target surface images using an image processor. The signal plot indicates that the model predicts the measured signal level adequately. The signal-to-noise plot indicates that the measured range limit of the imager occurs at about 70 m. The signal-to-noise plot shows two calculated curves that correspond to extremes in speckle noise. The low extreme assumes that the speckle is "correlated", meaning that there is little temporal motion in the grainy speckle pattern. The high extreme is calculated assuming that speckle is completely "uncorrelated" leading to random temporal variation of the speckle pattern. Decorrelation of speckle can result from target motion and atmospheric turbulence. At close ranges, only partial decorrelation of speckle is usually observed. This is the case in the pulsed imager range tests, as the measured curve can be seen to lie at the higher signal-to-noise end of the two extremes.

Tests of differential gas imaging were carried out as well. In differential imaging, the laser wavelength is switched between two values on a frame-to-frame timescale. One wavelength is set to be absorbed by the gas of interest (the "on" wavelength), the other is set to be transmitted (the "off" wavelength). Thus, collected frames will alternatively contain and not contain gas plume imagery.

These images are processed by taking the logarithm of the ratio of an on frame to the subsequent off frame. Prior to processing, the frames are normalized for laser pulse energy. The processing effectively calculates a laser absorbance spectrum of all pixels in the scene. This removes all scene information, leaving only the image of the gas plume. The differential imaging process can improve leak detection sensitivity because it allows small image contrast changes, due to small gas leaks, to be amplified over the image greyscale. Figure 7 shows the results of differential processing. At left is a single wavelength image containing a very small gas leak. At right is the same image processed in differential mode, leaving only the amplified gas plume image.

BENEFITS

The fundamental benefit offered by BAGI is the ability to instantaneously survey a large area for gas leaks. This should accelerate leak survey operations and, thus, reduce survey costs. A detailed cost/benefit analysis was conducted by LIS to estimate the cost savings (and price justification) of the instrument. The analysis treats the case of a distribution system leak survey for the natural gas industry. Note that this is only one example of an application of the imager. The relative cost of a leak search operation using the standard FID "sniffer" (as is being used now by a typical gas utility) was compared to the projected cost of the gas imaging approach using the scanned imager and the PPLN laser source. Key elements of this analysis are as follows:

- An imager field-of-view of 10° and a range of 70 m were assumed.
- The imager was assumed to be mounted in a van, viewing through a turret on the roof.
- The imaging van is assumed to stop at each residence and to travel with an average speed of 2.5 MPH between stops.
- The gas service spacing is assumed to be that of a dense suburban area, which is equal to 60 ft between services or 88 customers/mile
- It is assumed that a 100 mile-long distribution system is to be surveyed.
- It is assumed that 67% of the leaks are directly visible in the imager line-of-sight (i.e., not obscured by fences or bushes); it is assumed that the remaining leaks require point sensor attention by personnel.
- Time is allotted for the required classification of the strength and importance of leaks found (3 leaks are assumed to be found per mile).
- The instrument maintenance costs are included.
- Comparative cost analysis data for the conventional walking/mobile leak survey using FID sensors was obtained from a report by the Gas Research Institute and from Heath and Southern Cross. A walking survey is done by technicians with FID sensors to detect leaks in service pipelines in sidewalks, lawns, parkways, etc. A mobile survey is done with a truck-mounted FID unit for detection of leaks in mains under streets.

The results of the cost comparison is as follows:

Cost Comparison for the 100 Mile Distribution System Survey*

<u>ITEM</u>	<u>CURRENT TECHNOLOGY</u>	<u>IMAGER</u>
Survey time**:		
Mobile:	11.1 days	16.7 days
Foot:	18.3 days	16.7 days
Personnel required	5 technicians @ \$29/hr	2 technicians @ \$29/hr 1 driver @ \$20/hr
Survey costs	\$20,300	\$10,400
Operation & maintenance costs	\$6250/yr (5 FID units)	\$6478/yr (Imager + 2 FID units)

* 88 services/mile; mains + service lines = 184 miles; 1.69 leaks / mile

** For current technology, mobile is used for mains in streets and foot is used for all other locations (sidewalks, lawns, etc). For the imager, mobile refers to imager, foot is for locations for which there is not a direct line-of-sight.

The results indicate that, while the time required to do the survey is similar in each case, the net cost of the imaging approach is about 50% of that of the current approach. This results from the reduced manpower needs. If the imager was kept busy for 250 days per year, the cost savings is \$155,700 per year. The imager would pay for itself in just over 7 months. Cost/benefit analyses for other applications could be envisioned, but are beyond the scope of this document.

FUTURE WORK

During late May, 1997 the PPLN OPO will be coupled to the LIS scanner and the system will be field tested. The first tests will investigate its ability to detect above- and below-ground leaks at various standoff distances and leak rates. Following this, actual pipeline leaks will be viewed in a distribution system located in Atlanta, GA. Parallel tests will be made during the remainder of FY97 with the pulsed imaging system at Sandia and in local distribution systems in Livermore (as provided by PG&E). Although it is not proceeding to the prototype stage, imagery provided by the pulsed imager will provide data at higher image quality and resolution than the scanned system. It also provides the opportunity to field-test the differential imaging concept. Further advancements in differential imaging will also be made during FY97.

REFERENCES

1.T.J. Kulp, R. Kennedy, D. Garvis, T. McRae, and J. Stahovec, "The Development of an Active Imaging System and Its Application to the Visualization of Gas Clouds,," in *Proceedings of SPIE*,

Laser Applications in Meteorology and Earth and Atmospheric Remote Sensing (Society of Photo-Optical Instrumentation Engineers, Bellingham, WA, 1988), Vol. 1062, pp. 191-202.

2. T.J. Kulp, R. Kennedy, D. Garvis, L. Seppala, and D. Adomatis, "Further Advances in Gas Imaging," in Proceedings of the International Conference on Lasers '90 (Society for Optical and Quantum Electronics, McLean, VA, 1990), pp. 407-413 (1991).
3. T.G. McRae and T.J. Kulp, "Backscatter Absorption Gas Imaging — A New Technique for Gas Visualization," *Appl. Opt.* **32** 4037-4050 (1993).
4. T.J. Kulp, R. Kennedy, M. DeLong, D. Garvis, and J. Stahovec, "The Development and Testing of a Backscatter Absorption Gas Imaging System Capable of Imaging at a Range of 300-m," in *Proceedings of SPIE, Applied Laser Radar Technology* (Society of Photo-Optical Instrumentation Engineers, Bellingham, WA, 1993), Vol. 1936, pp. 204-212.

ACKNOWLEDGEMENTS

This work was conducted under support from the U.S. Department of Energy under contract number DE-AC04-94AL85000 through the National Petroleum Technology Office (Bartlesville, OK), and under support from the Gas Research Institute. The DOE contract representative is Dave Alleman. The GRI contract representative is Albert Teitsma.

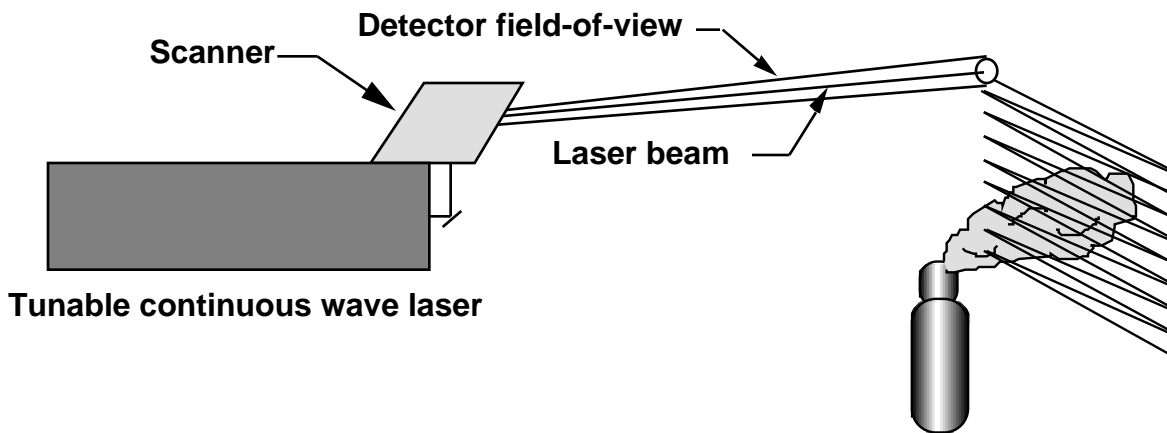


Figure 1 - Diagram of the scanned BAGI imager.

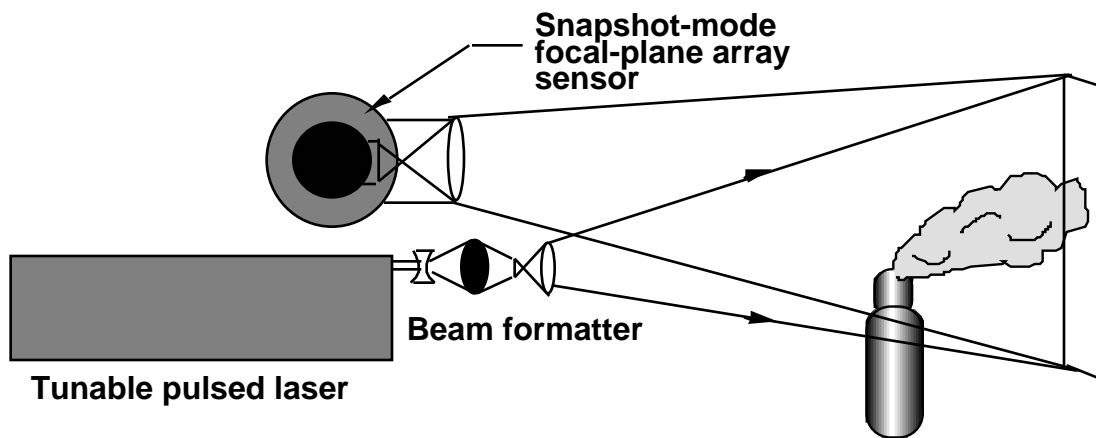


Figure 2 - Diagram of the pulsed BAGI imager.

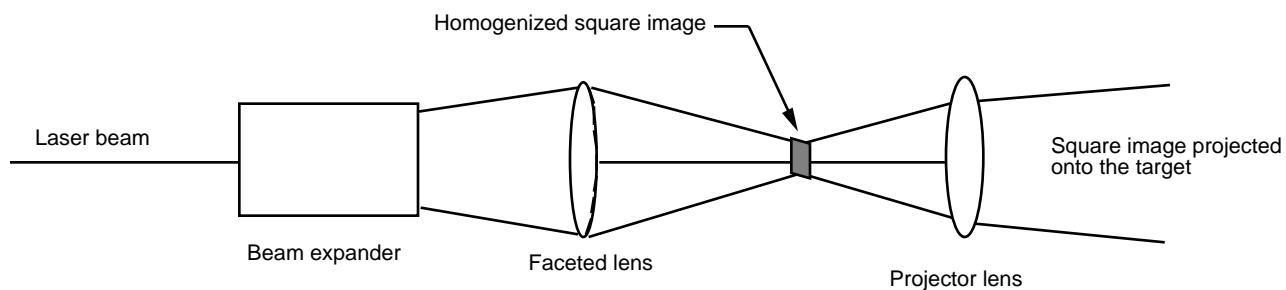


Figure 3 - Diagram of the beam formatter for the pulsed imager.

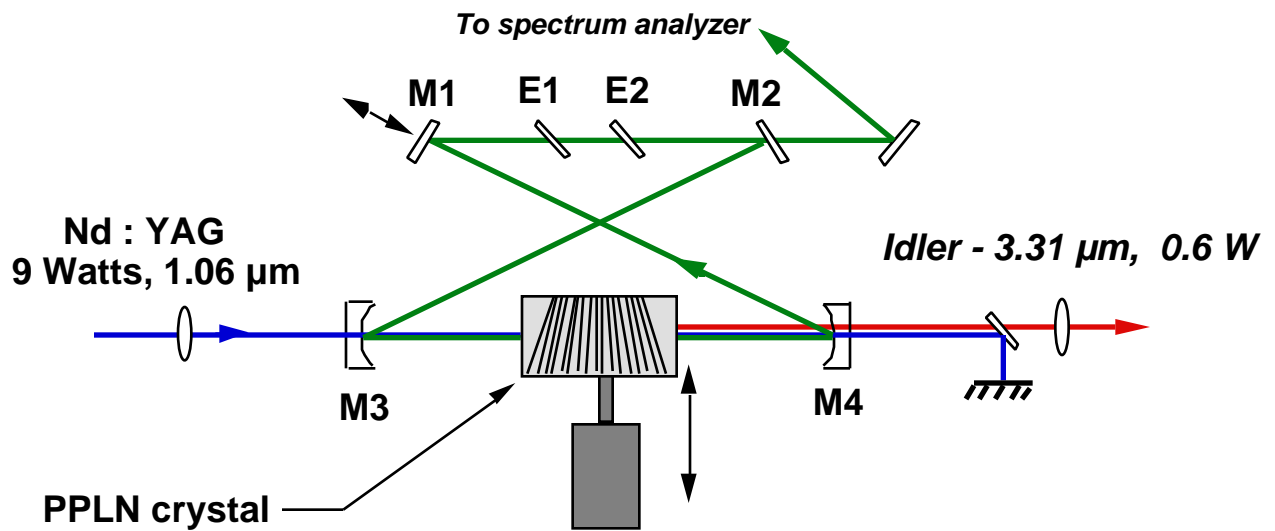


Figure 4 - Diagram of the PPLN OPO

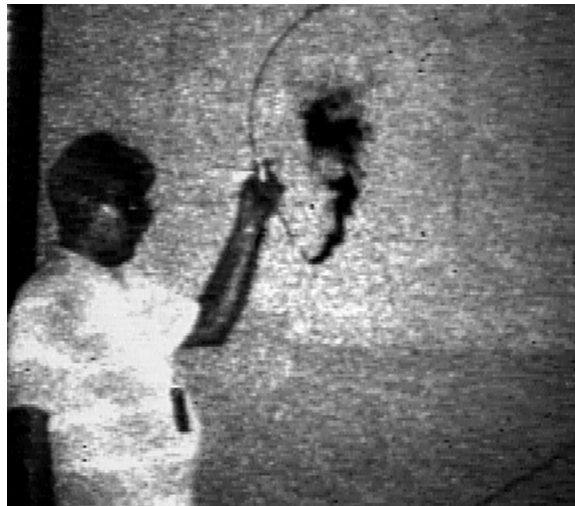


Figure 5 - Image taken with the pulsed BAGI imager at a range of 20 m. The gas is methane, being emitted at a flow rate of 0.2 standard cubic feet per hour (scfh).

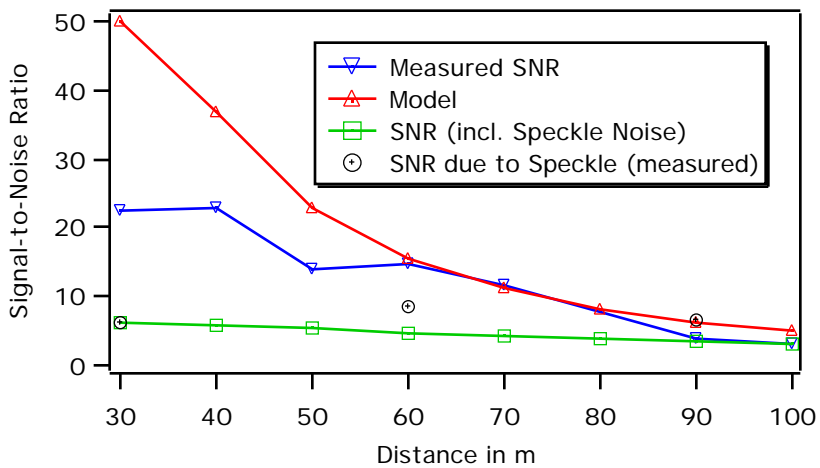
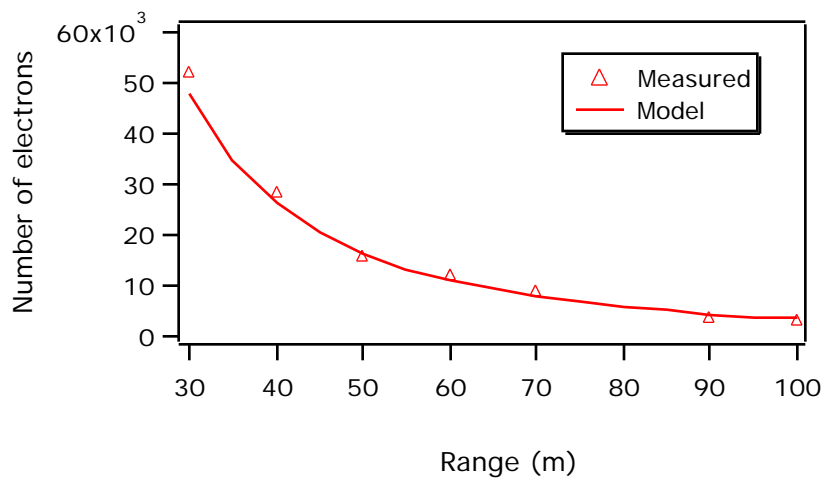


Figure 6 - Comparison of measured and calculated signal levels and signal-to-noise ratios. Above is a plot of the calculated and measured laser backscatter signal (in units of electrons at the detector). Below is the calculated and measured signal-to-noise ratio of the laser backscatter signal.

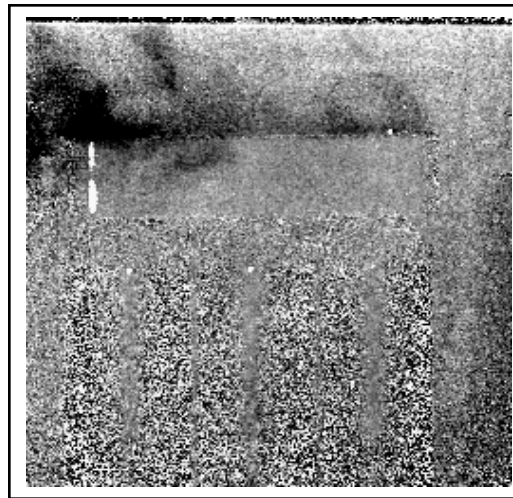
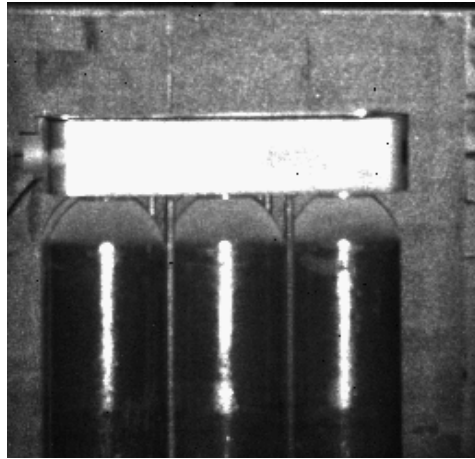


Figure 7 - Images illustrating BAGI detection in the differential mode. Above is a single-wavelength image containing a weak gas leak. Note that it is difficult to see the gas. Below is a processed differential image. There the image of the gas bottles has been removed, but the gas plume is clearly evident.